Supporting Information

Fuller et al. 10.1073/pnas.1323529111

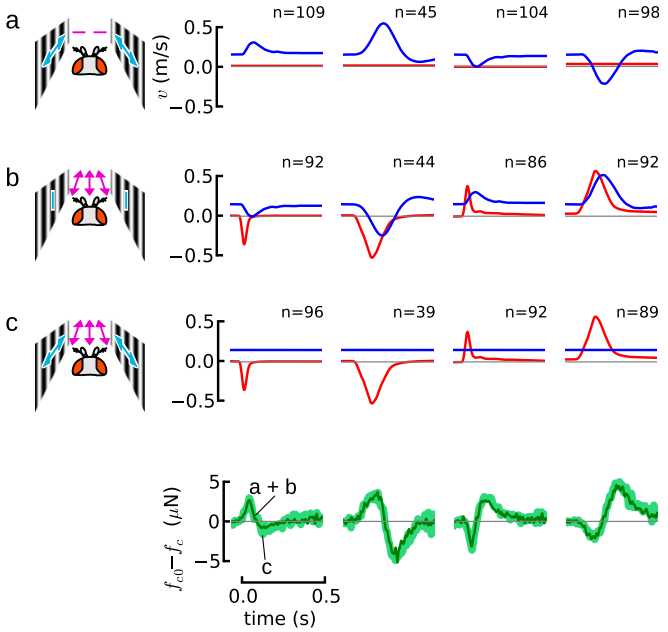

Fig. S1. Extension of Fig. 4 to include other rates of wind gust onset and polarity for (*A*) visual gusts, (*B*) wind gusts with reduced visual stimulus to probe the antenna response alone, and (*C*) naturalistic wind gusts in which both responses were stimulated simultaneously. The results suggest that in all cases, flies' control force output response, f_c, is a nearly ideal linear sum of the responses to each stimulus alone. See Fig. 4 legend for further details.

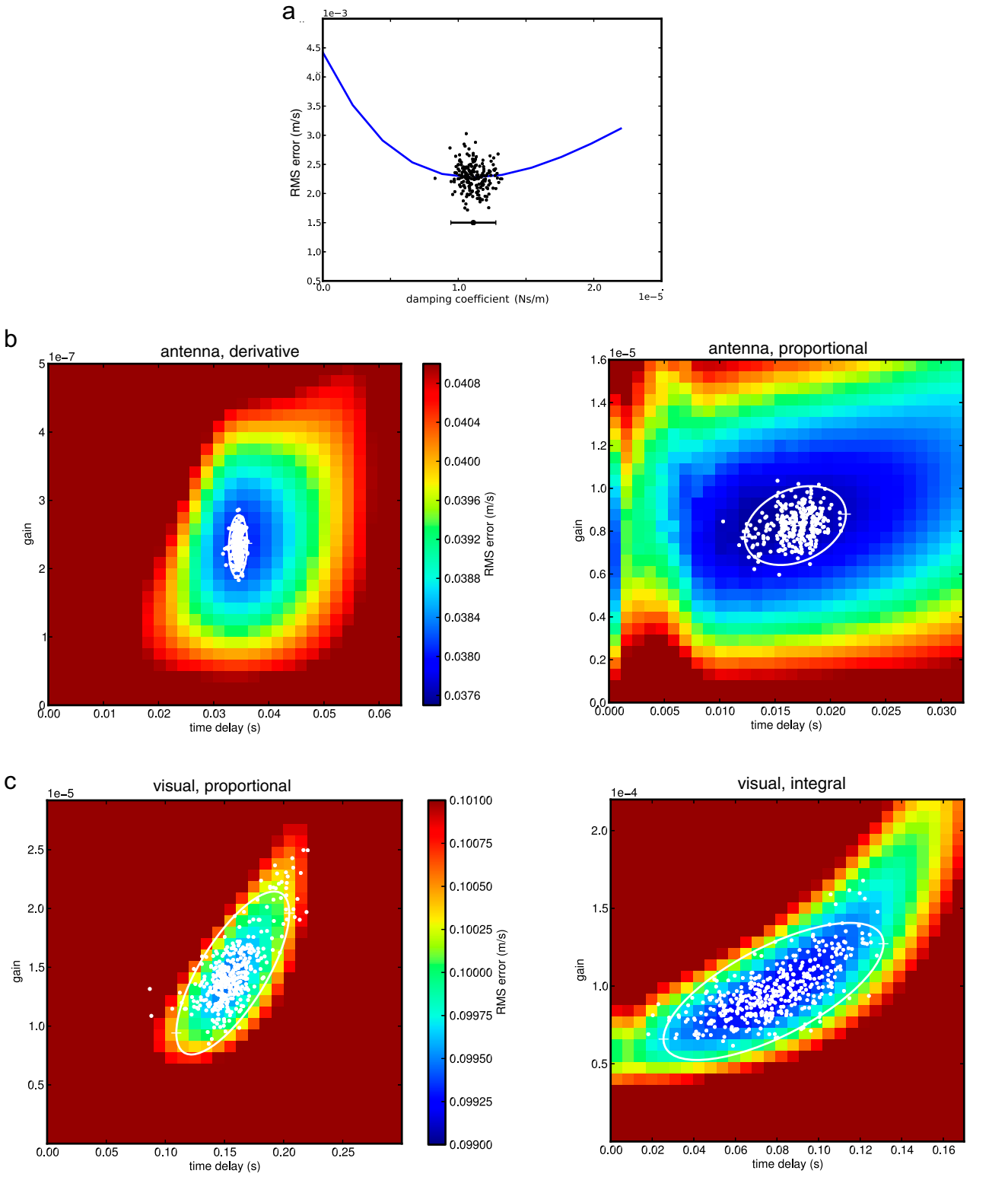

Fig. S2. Estimating parameter values and uncertainty envelopes. The complexity of our nonlinear parameter fit of multiple time-series trajectories suggested a bootstrapping approach (1). (*A*) Estimating the aerodynamic drag parameter b in Eq. **4**. We selected 300 resamples with replacement, to approximate resampling from the population, from the $n = 243$ collected trajectories. We performed a parameter fit for each resample using a nonlinear regression of the squared error (Eq. **10**) between groundspeed and the closed-loop prediction of groundspeed, using the prediction from Eq. **12**. The rms error for all trajectories (Eq. **10**) is plotted (line) along with parameter estimates vs. errors for each bootstrap sample (points). We estimated the parameter value and the 95% confidence interval by calculating the mean ± 1.96 times the SD of the bootstrap samples (shown as an error bar at the bottom). (*B*) Estimating gain K_a and time delay T_a of the antenna models in Eqs. **16** and **17**. For this nonlinear regression, we used Eq. **13** to calculate the groundspeed predictions. The number of parameters increased to two, so we show a color map of the rms error for all $n = 532$ trajectories collected (the same color map is used for both models; errors above a certain threshold are shown in the same color to better reveal structure near the minimum). Estimates for 400 bootstrap resamples are shown for each

Legend continued on following page

candidate model as white points. We calculated the parameter estimate by taking the mean of the bootstrap samples. To calculate 95% confidence intervals, we calculated the covariance matrix of the bootstrap estimates, calculated the singular values of this matrix, and set the width and height of the uncertainty ellipse to be 2×2.45 times the square root of these two singular values. This ellipse encloses approximately 95% of the bootstrap estimates. We used the two extremes of this ellipse (shown as +) as the range of the confidence interval because they represent the least stable (high gain, long delay) and most stable (low gain, short delay) extremes. Note that the marks do not appear to be at the extremes of these ellipses because of the unequal aspect ratio of the axes. (*C*) We used an equivalent procedure to estimate the gain K_v and time delay T_v for the visual feedback models in Eqs. **18** and **19**, using arista-ablated flies and Eq. **14** with $C_a = 0$ ($n = 250$).

1. Ljung L (1999) *System Identification* (Prentice Hall, Upper Saddle River, NJ).

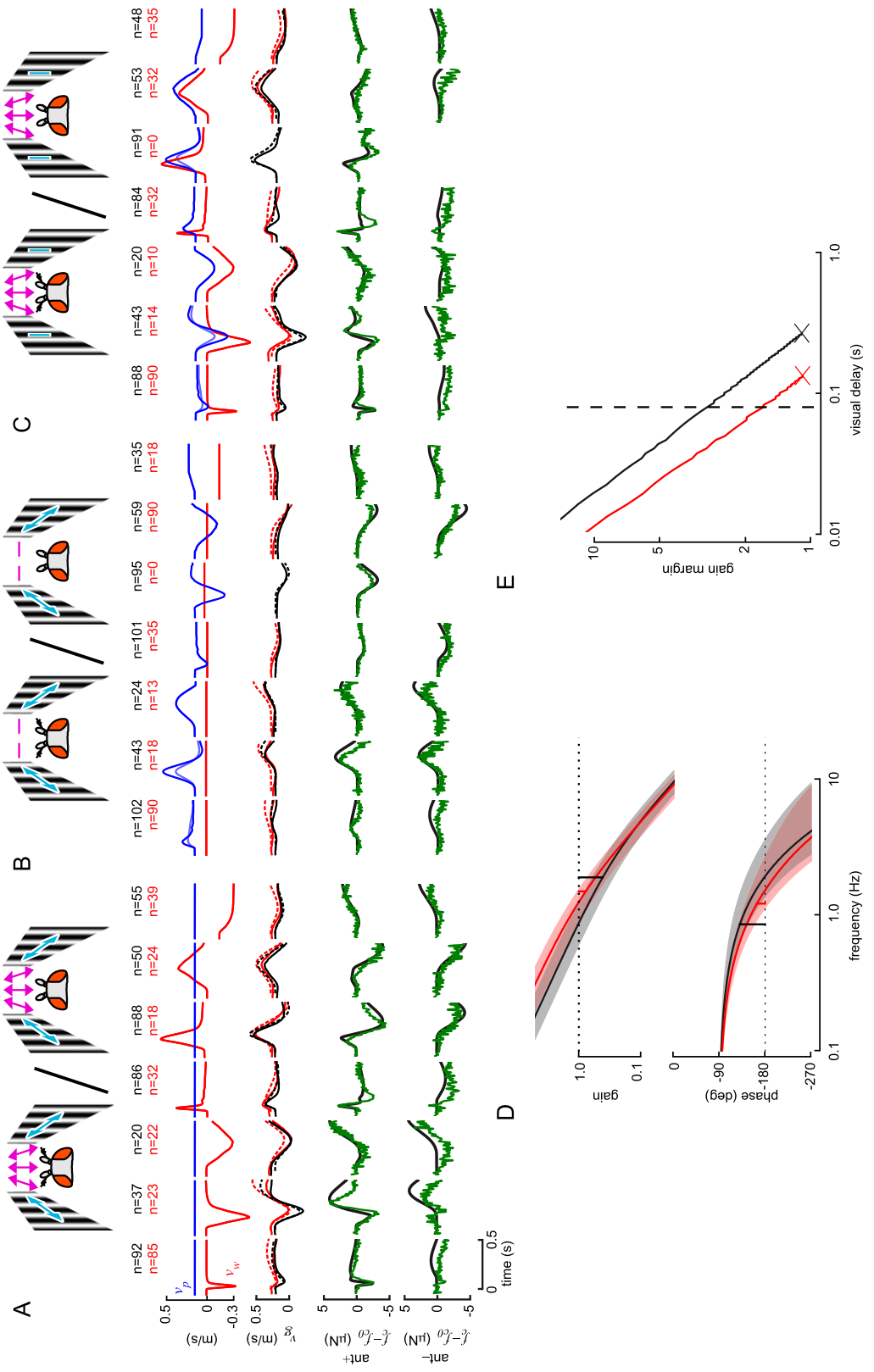

Fig. S3. Comparison of model and data for all conditions tested. Stimulus conditions are (*A*) wind gust, (*B*) visual gust, and (*C*) wind gust with low visual velocity. In faster gust conditions, the responses of arista-ablated flies were significantly different from those of intact flies, so we used different visual gusts (indicated by light blue for arista-ablated flies instead of dark blue) to best attenuate their visual input during the gust. Groundspeed responses are shown for intact flies (mean, black) and arista-ablated flies (red), with numbers of collected trajectories given in the corresponding color (n for intact flies is shown in top row). Dashed lines of corresponding color indicate the closed-loop output of the model simulated using Eq. **15**. We show the estimated control force output, f_c, that arises from visual and antenna responses for intact flies (ant$^+$) and arista-ablated flies (ant$^-$) (mean, jagged green line). Black lines indicate the simulated

Legend continued on following page

prediction of the fitted model. The transfer function from v_p to f_c used to produce these plots is Eq. **14** divided by $P(s)$; for the corresponding transfer function from v_w to f_c, define the transfer function in Eq. **13** as $G_{v_g v_w}(s)$, then the necessary transfer function is $(G_{v_g v_w}(s)/P(s)) - b$. For *C*, in which both wind velocity and projector velocity stimuli are presented, the plotted force prediction is the sum of the force predictions for each of the two sensory modes. (*D*) A magnitude/phase Bode plot of the loop transfer function (mean ± 95% confidence interval of bootstrap) broken at the visual feedback signal v_v shows that addition of antenna-mediated feedback increases gain and phase margins (length of vertical segments). (*E*) The addition of antenna feedback gives greater tolerance to longer visual feedback delay (× denotes onset of instability; dashed line shows the feedback delay estimated by model fitting).